



# Switchable and tunable erbium-doped fiber laser with the embedded Lyot filter

Xiang Gao<sup>1</sup> · Weihua Zhang<sup>1</sup> · Zhengrong Tong<sup>1</sup> · Xue Wang<sup>1</sup> · Lifang Xue<sup>1</sup> · Peng Li<sup>1</sup> · Junpeng Zhou<sup>1</sup> · Qiuhaohao Jiang<sup>1</sup> · Gangxiao Yan<sup>1</sup>

Received: 22 November 2022 / Accepted: 16 March 2023 / Published online: 3 April 2023  
© The Author(s), under exclusive licence to Springer-Verlag GmbH Germany, part of Springer Nature 2023

## Abstract

In this paper, a switchable and tunable erbium-doped fiber laser (EDFL) using an embedded Lyot filter is tested. The embedded Lyot filter based on a polarization-maintaining fiber (PMF) is theoretically analyzed and experimentally verified. By adjusting three polarization controllers (PCs), the output wavelengths in different wavelength states are emitted. By adjusting PC<sub>1</sub>, the output wavelengths can be switched among the single-wavelength output state and four different multi-wavelength output states, which are dual-, triple-, quad- and quintuple-wavelength outputs. In addition, the side-mode suppression ratio (SMSR) in this study can be up to ~53 dB. By adjusting PC<sub>2</sub> and PC<sub>3</sub> simultaneously, the output wavelengths show good tunability, and when in triple or quad-wavelength state, the wavelength interval is tunable.

## 1 Introduction

At present, based on the research of many scholars on lasers [1], it can be found that lasers have shown great promise in laser medicine, optical sensing and fiber telecommunication systems due to their good switching performance, flexible tuning, high output power and low cost. Comb filter plays an important role in the switchable and tunable fiber laser, such as Sagnac filter [6], Mach–Zehnder interferometer (MZI) [9], Lyot filter [12], Fabry–Perot interferometer [15] and so on. Up to now, a lot of researches have been done on erbium-doped fiber laser (EDFL) by scholars. Zijuan T et al. proposed a widely tunable EDFL. The innovation of the proposed fiber laser is to form an MZI by cascading a two-core photonic crystal fiber, which determines the tuning step and the interval of the output wavelengths. The tuning range can be from 1559.72 to 1593.54 nm [18]. Qi Z et al. proposed a switchable EDFL, which uses the parallel dual Lyot structure as a filter. The tuning range of single-wavelength

output is 13.52 nm. When the output is dual-wavelength or triple-wavelength, the output laser interval is tunable [19]. Qi Z et al. proposed a tunable EDFL, which uses the cascade structure as a filter. The tuning range has been greatly improved, and it is greater than 18 nm [20]. Bingsen H et al. proposed a tunable EDFL with the tuning ranges of 23 nm and 19 nm when the laser output wavelengths are single-wavelength and dual-wavelength, respectively, with the side-mode suppression ratio (SMSR) can be up to 57 dB [21].

In this study, an EDFL using the embedded Lyot as a filter is designed. Experiments show that the laser can switch the number of wavelengths and tune the output wavelengths. The innovative feature of the embedded Lyot filter used in this experiment is that two optical paths pass through the same section of polarization-maintaining fiber (PMF) and interfere. Compared with other fiber lasers, the SMSR in this work is high, which can be up to ~53 dB. The proposed fiber laser can be widely used in practice.

## 2 The device and principle of the filter

This chapter presents an analysis of the embedded Lyot filter. As shown in Fig. 1, the embedded Lyot filter consists of a polarizer, three polarization controllers (PCs), two 50:50 3 dB optical couplers (OCs), two three-port circulators, and a 4 m long PMF. After passing through the polarizer, the pump light turns into linearly polarized light. Then the linearly polarized

✉ Weihua Zhang  
nmgzwh@163.com

<sup>1</sup> Tianjin Key Laboratory of Thin Film Electronics and Communication Devices, Engineering Research Center for Optoelectronic Devices and Communication Technology of the Ministry of Education, School of Integrated Circuit Science and Engineering, Tianjin University of Technology, Tianjin 300384, People's Republic of China

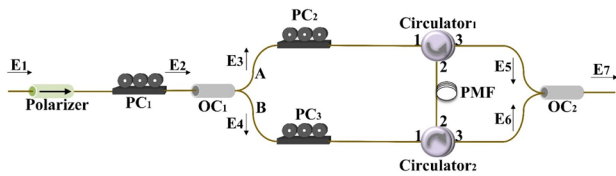


Fig. 1 Diagram of the embedded Lyot filter

Fig. 2 Simulation diagram of the embedded Lyot filter with (a) varying the angle  $\alpha$  of the polarized light (b) varying the phase delay  $\varphi_2$  and  $\varphi_3$  of the polarized light

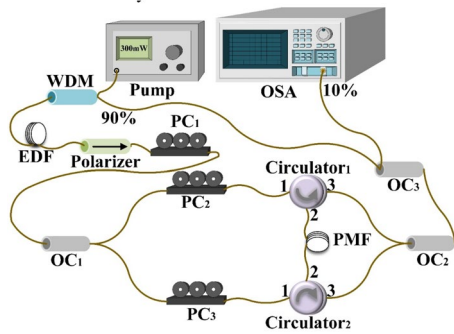
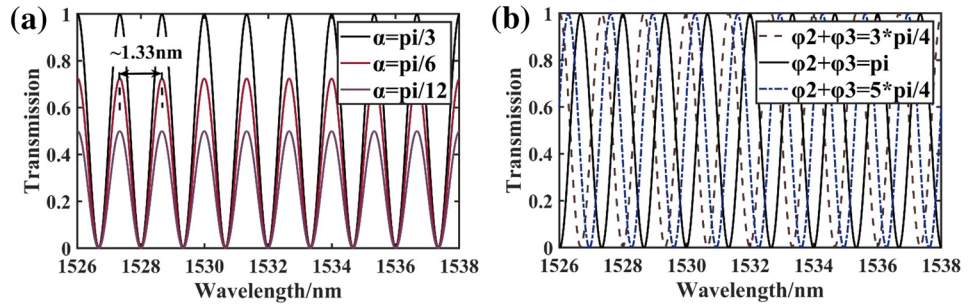


Fig. 3 Experimental structure diagram of EDFA with the embedded Lyot filter

light is transmitted to PC<sub>1</sub>, at which point the polarization state in the cavity changes. After coupling in OC<sub>1</sub>, the light splits into two beams of co-propagating light, branch A and branch B. After branch A passes through PC<sub>2</sub>, the polarization state in the cavity changes again. Branch A enters from port-1 of circulator<sub>1</sub> to port-2 of circulator<sub>1</sub>. Similarly, branch B travels in the same way. Branch A and branch B are output from port-2 of circulator<sub>1</sub> and port-2 of circulator<sub>2</sub> respectively to the same section of PMF and interfere. Branch A and branch B are then output from port-3 of circulator<sub>1</sub> and port-3 of circulator<sub>2</sub>, respectively. Finally, the two beams are coupled into OC<sub>2</sub> and interfere again at OC<sub>2</sub>.

The incident light is set to  $E_1$ . After passing through the polarizer, the pump light turns into linearly polarized light. Wavelength loss is minimized when the angle of polarization rotation of the light is in accordance with the angle of PC<sub>1</sub>. Thus, when the light in the cavity passes through PC<sub>1</sub>, an angle  $\alpha$  and a phase delay  $\varphi_1$  are introduced. According to the optical

waveguide theory, the light after passing through the PC<sub>1</sub> is denoted by  $E_2$ :

$$E_2 = \begin{bmatrix} \cos \alpha & \sin \alpha \\ -\sin \alpha & \cos \alpha \end{bmatrix} \begin{bmatrix} e^{-j\varphi_1} & 0 \\ 0 & e^{j\varphi_1} \end{bmatrix} E_1 \quad (1)$$

Light passing through OC<sub>1</sub> is divided into  $E_3$  and  $E_4$ . The coupling ratio of OC<sub>1</sub> is set to  $k_1$ , so that  $E_3$  and  $E_4$  are as follows:

$$\begin{bmatrix} E_3 \\ E_4 \end{bmatrix} = \begin{bmatrix} \sqrt{1-k_1} & j\sqrt{k_1} \\ j\sqrt{k_1} & \sqrt{1-k_1} \end{bmatrix} \begin{bmatrix} E_2 \\ E_2' \end{bmatrix}, \quad (2)$$

When light is transmitted to the PMF, the high birefringence effect is created, which enhances the mode selection effect. The transmission matrix of the PMF is as follows:

$$J_{PMF} = \begin{bmatrix} e^{-j\varphi_0} & 0 \\ 0 & e^{j\varphi_0} \end{bmatrix}, \quad (3)$$

where  $\varphi_0 = \frac{2\pi\Delta nL}{\lambda}$ .

The two beams output from port-3 of circulator<sub>1</sub> and port-3 of circulator<sub>2</sub> are set to  $E_5$  and  $E_6$  respectively, which can be described as the equation:

$$E_5 = \begin{bmatrix} e^{-j\varphi_0} & 0 \\ 0 & e^{j\varphi_0} \end{bmatrix} \begin{bmatrix} \cos \beta & \sin \beta \\ -\sin \beta & \cos \beta \end{bmatrix} \begin{bmatrix} e^{-j\varphi_2} & 0 \\ 0 & e^{j\varphi_2} \end{bmatrix} E_4 \quad (4)$$

$$E_6 = \begin{bmatrix} e^{-j\varphi_0} & 0 \\ 0 & e^{j\varphi_0} \end{bmatrix} \begin{bmatrix} \cos \gamma & \sin \gamma \\ -\sin \gamma & \cos \gamma \end{bmatrix} \begin{bmatrix} e^{-j\varphi_3} & 0 \\ 0 & e^{j\varphi_3} \end{bmatrix} E_3 \quad (5)$$

By adjusting PC<sub>2</sub> and PC<sub>3</sub>, the angle of polarization of the incident light with the fast axis of PMF changes, and

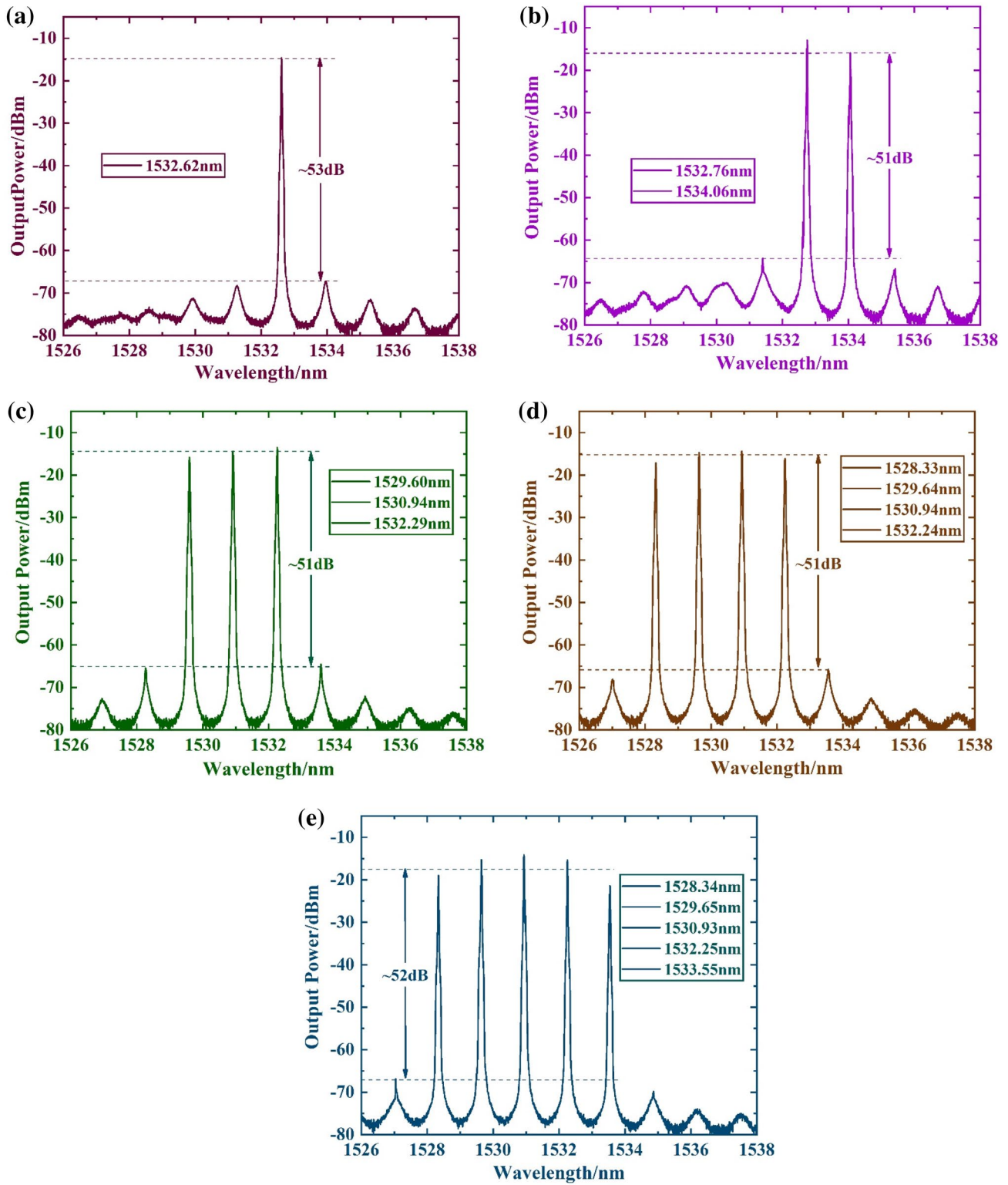


Fig. 4 Output spectra of a single- b dual- c triple- d quad- and e quintuple-wavelength outputs

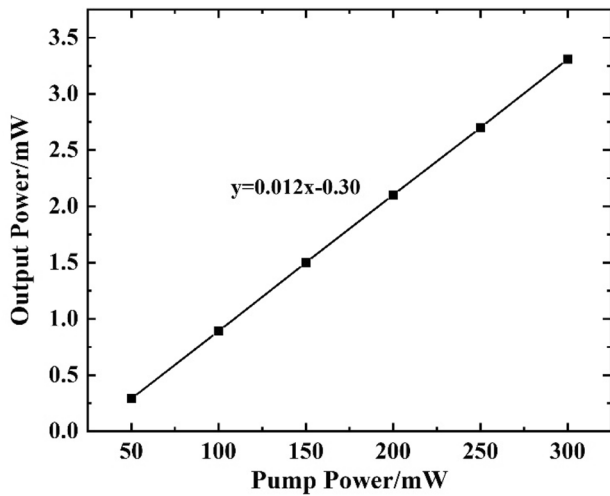


Fig. 5 Laser efficiency at the single-wavelength state

these angles are set to  $\beta$  and  $\gamma$ , respectively, and the phase delays introduced by  $PC_2$  and  $PC_3$  are set to  $\varphi_2$  and  $\varphi_3$ .  $E_5$  and  $E_6$  are transmitted output from  $OC_2$ ,  $E_7$  and  $E_7'$  can be calculated from

$$\begin{bmatrix} E_7 \\ E_7' \end{bmatrix} = \begin{bmatrix} \sqrt{1-k_2} & j\sqrt{k_2} \\ j\sqrt{k_2} & \sqrt{1-k_2} \end{bmatrix} \begin{bmatrix} E_5 \\ E_6 \end{bmatrix} \quad (6)$$

Finally, the transmission coefficient  $T$  is shown in formula (7).

$$T = \frac{|E_7|^2}{|E_1|^2} = \cos^2 \alpha \cdot \cos^2 (\beta - \gamma) + \sin^2 \alpha \cdot \sin^2 (\beta - \gamma) + 0.5 \times \sin 2\alpha \cdot \sin 2(\beta - \gamma) \cdot \cos^2 (\varphi_0 + \varphi_2 + \varphi_3) \quad (7)$$

It can be seen from formula (7) that the length of PMF, the angles of PCs and the phase delays by adjusting PCs determine the transmission coefficient  $T$  of the embedded Lyot filter. The simulation of the filter verifies the above theory, and the simulation results are shown in Fig. 2. For  $L = 4$ , the filter generates a comb spectrum with the wavelength interval of  $\sim 1.33$  nm.

To observe the transmission spectrum of the filter, a broadband light source (BBS, MCASE-CL-13-1-T1) and an optical spectrum analyzer (OSA, YOKOGAW A-AQ670D) are connected at the left and right ends of the filter shown in Fig. 1, respectively. The wavelength interval is  $\sim 1.33$  nm, which is the same as the wavelength interval obtained from the simulation analysis of the embedded Lyot filter.

### 3 Experimental results and discussion

Figure 3 shows the diagram of the experimental setup of the EDFL using the embedded Lyot as a filter. Firstly, the pump light from the 980 nm pump laser source passes through the 980/1550 nm wavelength division multiplexer (WDM). Then the pump light passes through a 7 m long erbium-doped fiber (EDF), which provides gain and achieves optical amplification. Secondly, the light passing through the EDF reaches the embedded Lyot filter shown in Fig. 1. The combined effect of the filter and polarization hole-burning (PHB) changes the gain and loss at different positions in the cavity and inhibits the mode competition in the cavity. Finally, after two interferences in the filter, the light is coupled into  $OC_3$ , 10% of the light is transmitted to OSA for observation and 90% of the light is transmitted back into the cavity.

Experiments are carried out at the pump power of 300 mW. Figure 4 shows the experimental results that the output wavelength can be switched among the single-wavelength output state and four different multi-wavelength output states by adjusting  $PC_1$ . As shown in Fig. 4 (a), the SMSR of the output wavelength can reach  $\sim 53$  dB. When the output wavelengths are dual-, triple-, quad- and quintuple-wavelength outputs as shown in Fig. 4b–e, the wavelength intervals are consistent with the simulation results of the filter shown in Fig. 1, which is  $\sim 1.33$  nm.

We measure the laser efficiency at the single-wavelength state. When the pump power is 48 mW, the output wavelength can be in a stable single-wavelength state. It can be seen from Fig. 5 that the output power is linearly related to the pump power and the laser efficiency is 1.2%. A comparison of the laser efficiency of our proposed fiber laser and the fiber laser with a laser efficiency of 0.05% presented in [20] shows that our proposed fiber laser has a higher efficiency.

By fixing the angle of  $PC_1$  and adjusting both  $PC_2$  and  $PC_3$  simultaneously, the output wavelengths are tunable. Figure 6 shows the tunable spectra of five different output wavelength states at constant pump power. The wavelength tuning ranges of single-, dual-, triple-, quad- and quintuple-wavelength outputs are  $\sim 5.31$  nm,  $\sim 4.87$  nm,  $\sim 4.69$  nm,  $\sim 3.92$  nm, and  $\sim 2.15$  nm, respectively, and the tuning step sizes are  $\sim 1.33$  nm,  $\sim 0.70$  nm,  $\sim 1.56$  nm,  $\sim 0.78$  nm and  $\sim 0.36$  nm. The experimental results validate the simulation analysis of the embedded filter in the previous chapter that the output wavelengths are tunable by adjusting  $PC_2$  and  $PC_3$ . As shown in Fig. 6a, it is observed that the SMSRs of the single-wavelength outputs on both sides are lower than the middle. The reason for this phenomenon is that the output power on both sides of the gain spectrum of EDF used in the experiment is lower than the output power in the middle. When the laser on both sides

**Fig. 6** Tunable output spectra of **a** single- **b** dual- **c** triple- **d** quad- and **e** quintuple-wave-length outputs

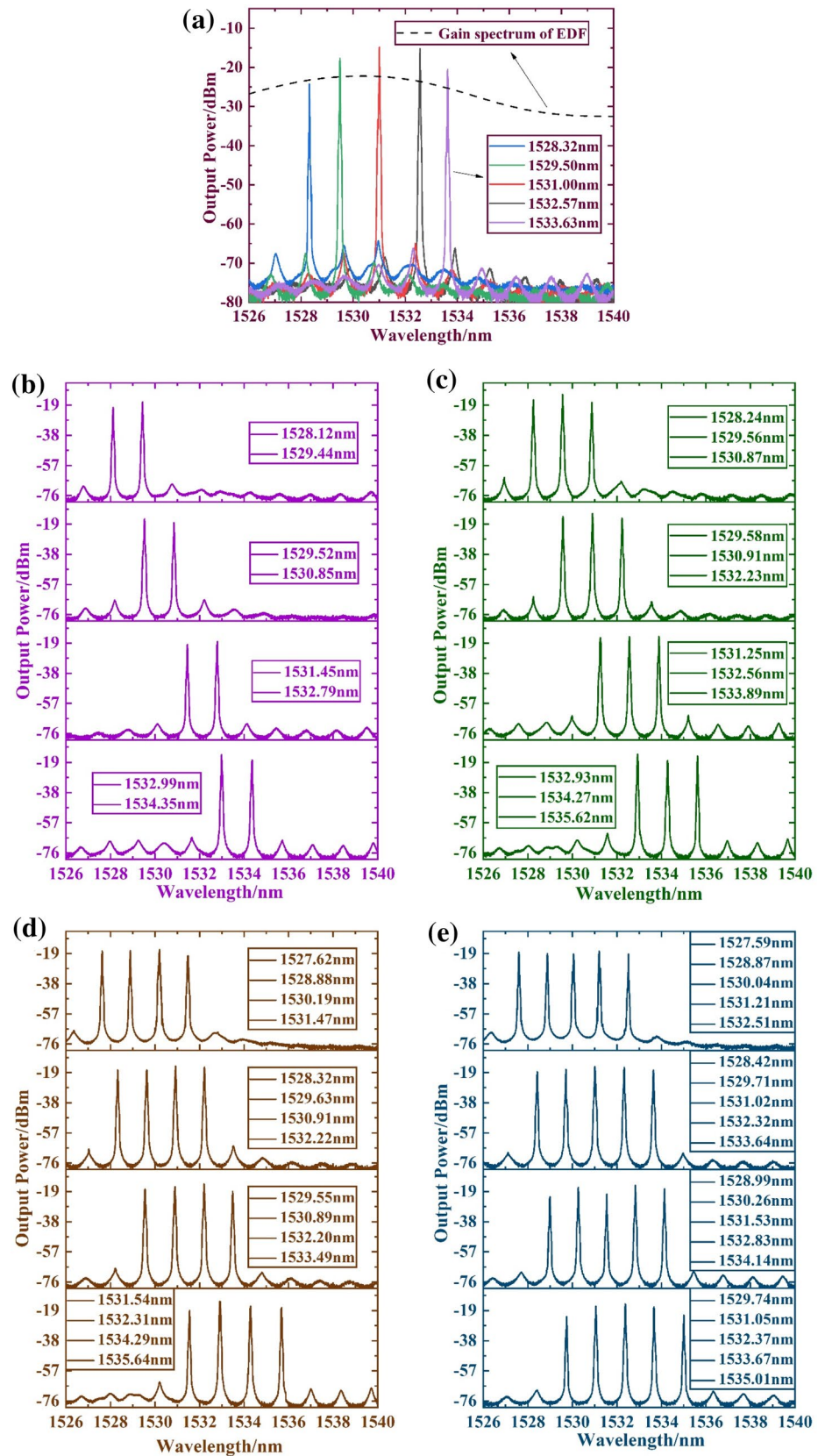


**Fig. 7** Spectra of the triple-wavelength output states with (a), (b) and (c) different intervals

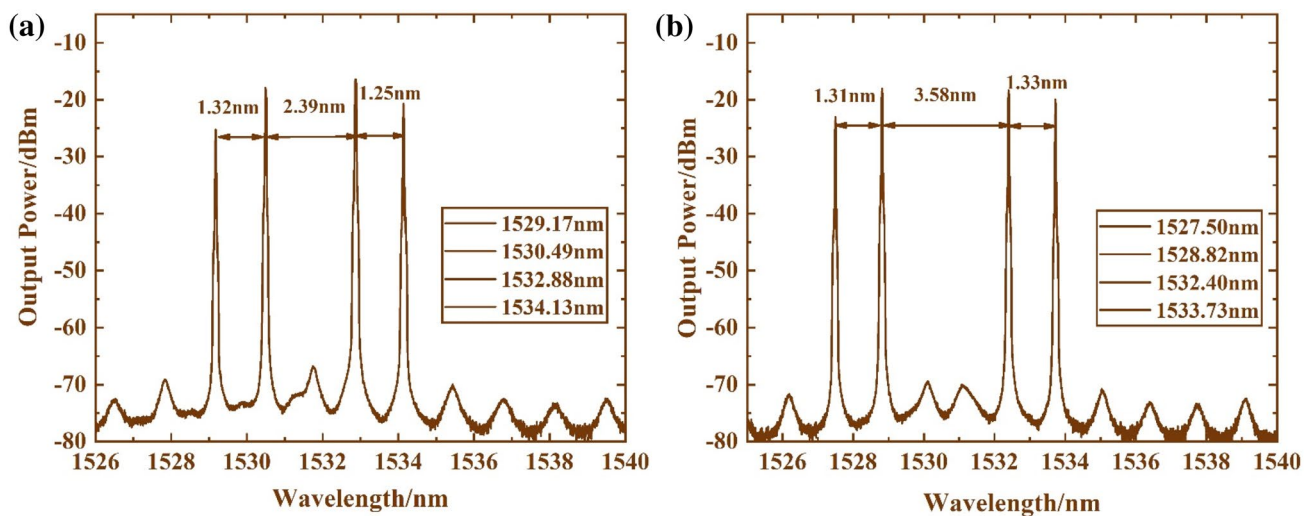
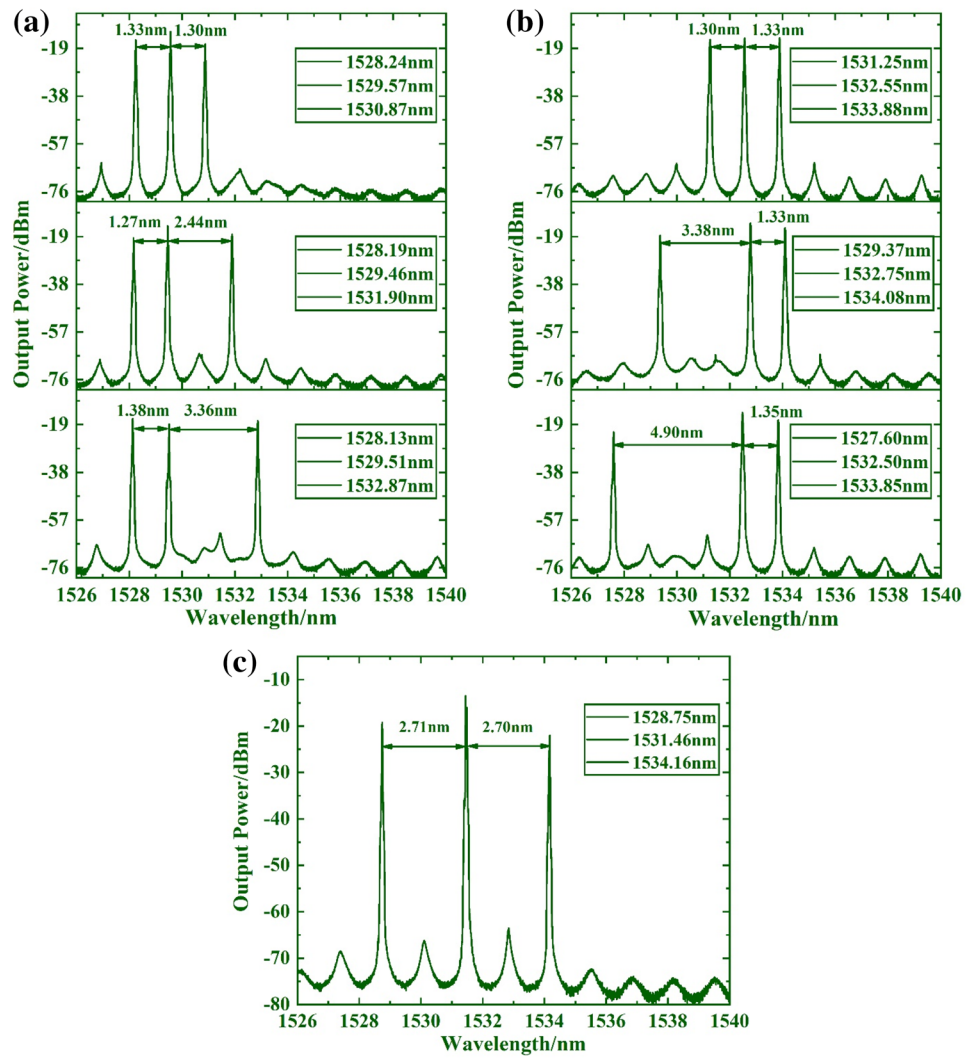


**Fig. 8** Spectra of the quad-wavelength output states with (a) and (b) different intervals

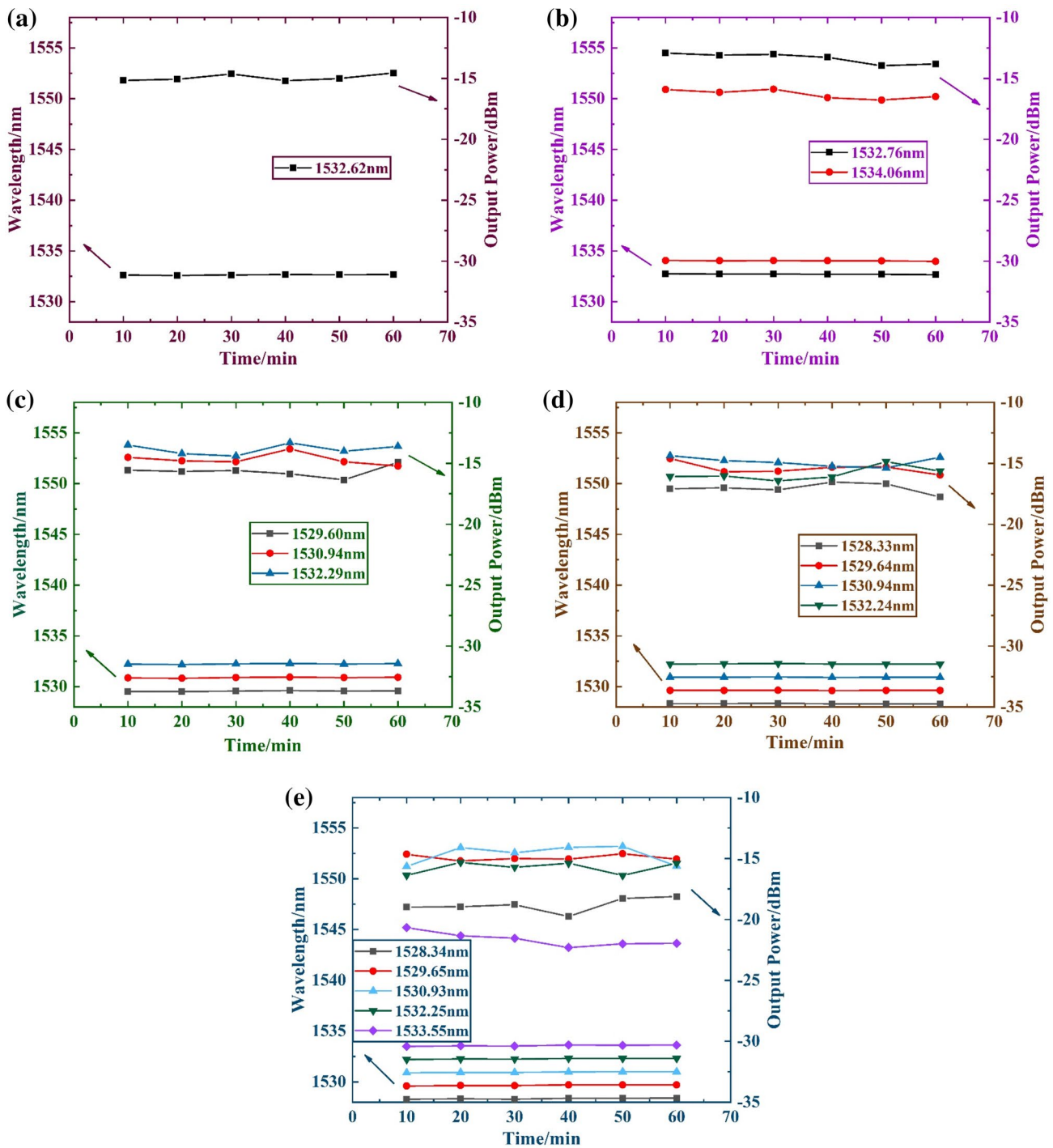


Fig. 9 Power fluctuations and wavelength drifts of a single- b dual- c triple- d quad- and e quintuple-wavelength outputs

is excited, the output wavelength is suppressed because the loss at this position is greater than the gain.

In addition to tuning the output wavelength, our proposed fiber laser can also change the wavelength interval by simultaneously adjusting PC<sub>2</sub> and PC<sub>3</sub>, when the output wavelength is triple- or quad-wavelength. The output

spectra of the triple-wavelength output states are shown in Fig. 7.

Figure 8 shows the output spectra of the quad-wavelength output states. We believe that this phenomenon is due to the combined effect of the filter and PHB. In the process of adjusting PC<sub>2</sub> and PC<sub>3</sub>, the state of the output wavelength changes. The wavelength interval changes

**Table 1** Comparison of this work with other work on fiber lasers

The structure of the filter	Max wavelength number	Threshold Power	SMSR					References
			Single	Dual	Triple	Quad	Quintuple	
Mach–Zehnder interferometer employing seven-core fiber	2	73mW	> 25.4	> 10.2	-	-	-	[22]
Parallel-structured Lyot filter	3	-	~44	~45	~45	-	-	[19]
The cascaded filters	7	-	47	43	43	42	40	[20]
Balloon-like interferometer structure-based comb-filter	4	75mW	30.3	26.47	> 30.2	> 31.5	-	[4]
The embedded Lyot filter	5	~48mW	~53	~51	~51	~51	~52	This work

when the laser cavity is in a specific polarization state. In summary, the fiber laser has good switchability and flexible tunability.

As shown in Fig. 9, the laser outputs are tested every 10 min at room temperature for 60 min to study the stability of the fiber laser. The experimental results show that the fluctuations of wavelength and peak power are less than 0.12 nm and 1.64 dB respectively, which verifies that the EDFL has good stability.

In the end, we compare the EDFL in this work with other switchable and tunable fiber lasers. As shown in Table 1, the maximum number of output wavelength, threshold power and the SMSR of the laser are listed. It is noted that the SMSR of the output wavelength in this work is higher than others. It has promising applications in optical communications, high-precision sensing and coherent detection.

## 4 Conclusions

In this paper, we propose a switchable and tunable EDFL with the embedded Lyot filter. The innovation of the fiber laser is that the two beams of light pass through the same section of PMF. The laser working threshold is ~48 mW and the laser efficiency is 1.2%. The output wavelength can be switched by adjusting  $PC_1$ . By adjusting  $PC_2$  and  $PC_3$  simultaneously, the fiber laser shows good tunability. The proposed EDFL has the advantages of high SMSR, high laser efficiency, good stability and low cost. Therefore, the fiber laser proposed in this paper has great potential applications in fiber communication, optical sensing and other fields. In future work, we will optimize the filter and improve the performance of the fiber laser.

**Acknowledgements** This work is supported by the National Natural Science Foundation of China (Grant number 61974104), National Youth Natural Science Foundation of China (Grant number 62205245), National Natural Science Foundation of China (Grant number 62003237) and Tianjin Enterprise Technology Commissioner Project (Grant number 20YDTPJC01700).

**Author contributions** WZ and ZT guided the experimental research, provided experimental equipment and laboratory, and guided and revised the manuscript. XG mainly conducted experimental research and wrote manuscript text, and processed all experimental data. XW, LX and PL made corrections to the manuscript and provided funds to buy experimental equipment. JZ, QJ and GY assisted in the operation of the experiment.

**Funding** Xue Wang, 62205245, Lifang Xue, 61974104, Peng Li, 62003237.

**Data Availability** The datasets generated and analysed during the current study are available from the corresponding author on reasonable request.

## Declarations

**Conflict of interest** There is no conflict to declare.

## References

1. Y.B. Chang, L. Pei, T.G. Ning, J.J. Zheng, Switchable multi-wavelength fiber laser based on hybrid structure optical fiber filter. *Opt. Laser Technol.* **124**, 105985 (2020). <https://doi.org/10.1016/j.optlas.2019.105985>
2. Y. Li, Z.L. Xu, Y.Y. Luo, Y. Xiang, Z.J. Yan, D.M. Liu, Q.Z. Sun, Tunable multiwavelength fiber laser based on a  $\theta$ -shaped microfiber filter. *Appl. Phys. B.* **124**, 109 (2018). <https://doi.org/10.1007/s00340-018-6979-9>
3. Y.B. Chang, L. Pei, T.G. Ning, J.J. Zheng, J. Li, C.J. Xie, Switchable and tunable multi-wavelength fiber ring laser employing a cascaded fiber filter. *Opt. Fiber Technol.* **58**, 102240 (2020). <https://doi.org/10.1016/j.yofte.2020.102240>
4. H.Q. Merza, S.K. Al-Hayali, A.H. Al-Janabi, Tunable full waveband- and adjustable spacing multi-wavelength erbium-doped fiber laser based on controlling cavity losses through bending sensitive interferometric filter. *Infrared Phys. Technol.* **116**, 103791 (2021). <https://doi.org/10.1016/j.infrared.2021.103791>
5. X. Liu, M. Pang, Revealing the buildup dynamics of harmonic mode-locking states in ultrafast lasers. *Opt. Laser Technol.* **13**, 1800333 (2019). <https://doi.org/10.1002/lpor.201800333>
6. W. He, L.Q. Zhu, M.L. Dong, F. Luo, Tunable and switchable thulium-doped fiber laser utilizing Sagnac loops incorporating two-stage polarization maintaining fibers. *Opt. Fiber Technol.* **29**, 65–69 (2016). <https://doi.org/10.1016/j.yofte.2016.03.003>
7. X.D. Liu, S.Q. Lou, Z.J. Tang, Y.X. Zhou, H.Z. Jia, P. Sun, Tunable dual-wavelength ytterbium-doped fiber ring laser based on



- a Sagnac interferometer. *Opt. Laser Technol.* **116**, 37–42 (2019). <https://doi.org/10.1016/j.optlastec.2019.03.006>
8. T. Li, F.P. Yan, D. Cheng, Q. Qin, Y. Guo, T. Feng, Z.Y. Bai, X.M. Du, Y.P. Suo, H. Zhou, Switchable multi-wavelength thulium-doped fiber laser using a cascaded or two-segment sagnac loop filter. *IEEE Access.* **10**, 13026–13037 (2022). <https://doi.org/10.1109/ACCESS.2022.3146414>
  9. J.A. Martin-Vela, J.M. Sierra-Hernandez, E. Gallegos-Arellano, J.M. Estudillo-Ayala, M. Bianchetti, D. Jauregui-Vazquez, J.R. Reyes-Ayona, E.C. Silva-Alvarado, R. Rojas-Laguna, Switchable and tunable multi-wavelength fiber laser based on a core-offset aluminum coated Mach-Zehnder interferometer. *Opt. Laser Technol.* **125**, 106039 (2020). <https://doi.org/10.1016/j.optlastec.2019.106039>
  10. E.C. Silva-Alvarado, A. Martinez-Rios, E. Gallegos-Arellano, J.A. Martin-Vela, L.M. Ledesma-Carrillo, J.R. Reyes-Ayona, T.E. Porraz-Culebro, J.M. Sierra-Hernandez, Tunable filter based on two concatenated symmetrical long period fiber gratings as Mach-Zehnder interferometer and its fiber lasing application. *Opt. Laser Technol.* **149**, 107824 (2022). <https://doi.org/10.1016/j.optlastec.2021.107824>
  11. H. Ahmad, S.I. Ooi, Z.C. Tiu, 100 GHz free spectral range-tunable multi-wavelength fiber laser using single–multi–single mode fiber interferometer. *Appl. Phys. B.* **125**, 99 (2019). <https://doi.org/10.1007/s00340-019-7209-9>
  12. Y.J. Zhu, Z.K. Cui, X.N. Sun, T.K.M. Shirahata, L. Jin, S.J. Yamashita, S.Y. Set, Fiber-based dynamically tunable Lyot filter for dual-wavelength and tunable single-wavelength mode-locking of fiber lasers. *Opt. Express.* **28**, 27250–27257 (2020). <https://doi.org/10.1364/OE.402173>
  13. M.S.K. Jamalul, A.H. Sulaiman, F. Abdullah, N. Zulkifli, M.T. Alresheedi, M.A. Mahdi, N.M. Yusoff, Selectable multiwavelength thulium-doped fiber laser based on parallel Lyot filter. *Opt. Fiber Technol.* **70**, 102892 (2022). <https://doi.org/10.1016/j.yofte.2022.102892>
  14. L.Y. Xin, X.F. Zhou, J.L. Chen, Low threshold multi-wavelength erbium-doped fiber ring laser with NOLM and Lyot filter. *Opt. Fiber Technol.* **68**, 102800 (2022). <https://doi.org/10.1016/j.yofte.2021.102800>
  15. X. Wang, T.W. Chen, D.L. Meng, F. Wang, A simple FBG Fabry-Perot sensor system with high sensitivity based on fiber laser beat frequency and vernier effect. *IEEE sensors J.* **21**, 71–75 (2021). <https://doi.org/10.1109/JSEN.2020.2974501>
  16. J.M. Estudillo-Ayala, D. Jauregui-Vazquez, J.W. Haus, M. Perez-Maciel, J.M. Sierra-Hernandez, M.S. Avila-Garcia, R. Rojas-Laguna, Y. Lopez-Diequez, J.C. Hernandez-Garcia, Multi-wavelength fiber laser based on a fiber Fabry-Perot interferometer. *Appl. Phys. B.* **121**, 407–412 (2020). <https://doi.org/10.1007/s00340-015-6265-z>
  17. X.L. Guo, F. Xie, Z.C. Guo, X.Y. Zhang, Research on multi-wavelength single-longitudinal mode optical fiber laser with FBG and FBG based Fabry-Perot filter. *Opt. Fiber Technol.* **66**, 102639 (2021). <https://doi.org/10.1016/j.yofte.2021.102639>
  18. Z.J. Tang, S.Q. Lou, X. Wang, Stable and widely tunable single-/dual-wavelength erbium-doped fiber laser by cascading a twin-core photonic crystal fiber based filter with Mach-Zehnder interferometer. *Opt. Laser Technol.* **109**, 249–255 (2019). <https://doi.org/10.1016/j.optlastec.2018.07.060>
  19. Q. Zhao, L. Pei, J.J. Zheng, M. Tang, Y.H. Xie, J. Li, T.G. Ning, Switchable multi-wavelength erbium-doped fiber laser with adjustable wavelength interval. *J. Lightwave Technol.* **37**, 3784–3790 (2019). <https://doi.org/10.1109/JLT.2019.2920840>
  20. Q. Zhao, L. Pei, J.J. Zheng, M. Tang, Y.H. Xie, J. Li, T.G. Ning, Tunable and interval-adjustable multi-wavelength erbium-doped fiber laser based on cascaded filters with the assistance of NPR. *Opt. Laser Technol.* **131**, 106387 (2020). <https://doi.org/10.1016/j.optlastec.2020.106387>
  21. B.S. Huang, X.Z. Sheng, Z.J. Tang, S.Q. Luo, High SMSR and widely tunable multi-wavelength erbium doped fiber laser based on cascaded filters. *Infrared Phys. Technol.* **122**, 104082 (2022). <https://doi.org/10.1016/j.infrared.2022.104082>
  22. W. He, W. Zhang, L. Zhu, X. Lou, M. Dong, C-band switchable multi-wavelength erbium-doped fiber laser based on Mach-Zehnder interferometer employing seven-core fiber. *Opt. Fiber Technol.* **46**, 30–35 (2018). <https://doi.org/10.1016/j.yofte.2018.08.011>

**Publisher's Note** Springer Nature remains neutral with regard to jurisdictional claims in published maps and institutional affiliations.

Springer Nature or its licensor (e.g. a society or other partner) holds exclusive rights to this article under a publishing agreement with the author(s) or other rightsholder(s); author self-archiving of the accepted manuscript version of this article is solely governed by the terms of such publishing agreement and applicable law.